CEBAF Program Advisory Committee Eight Cover Sheet

This proposal must be received by close of business on Thursday, April 14, 1994 at:

CEBAF
User Liaison Office, Mail Stop 12 B
12000 Jefferson Avenue
Newport News, VA 23606

Proposal Title

A Study of Off-Shell Effects in EM Reactions

Contact Person

Name: Johannes van den Brand
Institution: NIKHEF / UW-Madison
Address: Kruislaan 409
Address: P.O. Box 41882
City, State ZIP/Country: Amsterdam, 1009 dB, The Netherlands
Phone: 31-20-5922142 **FAX:** 31-20-5922165
E-Mail → Internet: jo@paramount.nikhefk.nikhef.nl

Experimental Hall: A
Total Days Requested for Approval: 20
Minimum and Maximum Beam Energies (GeV): 2.5 - 4.0
Minimum and Maximum Beam Currents (μAmps): 25 - 100 μA

CEBAF Use Only

Receipt Date: _____

By: _____

A Study of
Off-Shell Effects in Electromagnetic Reactions

Submitted by

J.F.J. van den Brand* (Co-spokesman), J. Blouw, C.W. de Jager, T. Henkes
J. Koch, M. Kolstein, L. Lapikás, H. Poolman, P.K.A. de Witt Huberts and H. de Vries
NIKHEF-K, Amsterdam, The Netherlands
E-mail: jo@paramount.nikhefk.nikhef.nl
Ph.: 31-20-592-2015 Fax.: 31-20-592-2165

H.J. Bulten (Co-spokesman), M. Miller, O. Unal and Z.L. Zhou
Department of Physics, University of Wisconsin, Madison

R. Ent (Co-spokesman), O.K. Baker*, D. Mack, R. Michaels, J. Mitchell,
A. Saha and L. Tang*
Department of Physics, CEBAF, Newport News
* *and jointly, Hampton University, Hampton, Virginia*

H.P. Blok
Free University, Amsterdam, The Netherlands

S. Pollock
University of Colorado, Boulder, Colorado

R. Alarcon
Arizona State University, Tempe, Arizona

T.P. Welch
Oregon State University, Corvallis, Oregon

J.M. Finn
College of William and Mary, Williamsburg, Virginia

Exp. No.	Description	Beam Hours	Energy	Current	D.F.
	^{1}H$(\vec{e}, e'\vec{p})\gamma$	480	2.5 - 4 GeV	100 μA	100 %

ABSTRACT

We propose a study of the off-shell electron-proton vertex through a measurement of the virtual Compton scattering cross section and polarization transfer coefficients in the reaction $^1\mathrm{H}(\vec{e},e'\vec{p})\gamma$. Our proposed measurement will determine the dependence of these observables both as a function of the four-momentum transfer, over the range of 0.28 to 1.00 $(\mathrm{GeV/c})^2$, and as a function of invariant mass of the intermediate state in the range of 938 to about 1150 MeV. The experiment exploits the 100 % duty factor electron beam at CEBAF in combination with the proton polarimeter, which is presently being developed for Hall A by a collaboration of the College of William and Mary, and Rutgers University. The combined knowledge of electron and proton spin enables a precise structure-function separation. The proposed experimental method allows a separation with small systematic error, as for each such measurement only one electron beam energy is used and the kinematical configuration is fixed.

Recent calculations using microscopic models for the nucleon predict that the form factors of the off-shell proton differ significantly from the on-shell form factors. In addition, a correct description of the vertex requires the existence of additional vertex operators and associated form factors, beyond $\mathrm{F_1(Q^2)}$ and $\mathrm{F_2(Q^2)}$. The proposed experimental method allows one to test models for the off-shell behavior under very clean circumstances. This is in contrast to the situation for electron scattering from off-shell nucleons bound in a nucleus, where one is faced with obscurance due to e.g. nuclear-structure, final-state interaction and meson-exchange currents effects.

Using a separable model, we present estimates for the cross section and the polarization transfer coefficients, D_{lt} and D_{ll}, including contributions from electron and proton radiation, as well as the interference contribution. For the measurements probing the dependence of the cross section as a function of the four-momentum transfer, we expect better than 2 % statistical precision within 80 hours of beam time. It is shown that the coefficients D_{ll} and D_{lt} can be determined to an accuracy better than 0.03 within 350 hours of beam time. This experiment requires forward electron scattering angles in order to enhance the $^1\mathrm{H(e,e'p)}\gamma$ cross section. The excellent resolution of the Hall A spectrometer setup is necessary in order to cleanly select virtual Compton scattering events.

Table of Contents

I. Introduction

As one of the basic motivations for using electron scattering as a probe of hadronic currents it is generally stated[1,2] that the electromagnetic interaction is well understood and precisely calculable from QED. This statement is certainly correct for the electron-photon part of the interaction, but it does not apply at the same level of precision to the photon-hadron coupling. Although the interaction of a virtual photon to a free nucleon has been precisely measured in electron scattering, almost nothing is known about the coupling of a virtual photon to a virtual nucleon, i.e. a nucleon off its mass shell. The main difficulty is that a complete understanding of the dynamical structure of the nucleon is required in order to calculate its off-shell electromagnetic interaction. (Presently, even no field-theoretical model exists for the free nucleon which describes the measured Dirac and Pauli form factors correctly). Therefore, it is common practice to use ad-hoc recipes[3] which basically express the off-shell properties in terms of free nucleon information. This was done when describing the electromagnetic interaction of a nucleon bound in a nucleus.

When a nucleon is embedded in a nucleus several interesting phenomena appear which need to be understood. Firstly, the bound nucleon is necessarily off-shell and the uncertainties discussed above directly apply to this case. Secondly, one faces the possibility of genuine, density-dependent medium effects[4], such as quark-exchange contributions[5,6] and meson-exchange currents. Furthermore, the electromagnetic coupling to the bound nucleon is dependent on the nuclear dynamics[7] through the self-energy of the nucleon in the nuclear medium. In the last decade, many experiments have been performed in kinematic regimes where lepton scattering from a bound nucleon is expected to be the dominant process. Large discrepancies are observed[8-10] when these data are analyzed using current operators based on the *free* nucleon observables. At the moment a conclusive explanation of the observations is not available.

In this proposal we argue that one should first understand the treatment of the full off-shell electromagnetic vertex of a single nucleon, before considering any interpretation of a bound nucleon. We therefore propose a study of the off-shell electron-proton vertex through a measurement of virtual Compton (VC) scattering, i.e. the reaction $^1\mathrm{H}(\vec{e},e'\vec{p})\gamma$. Our proposed measurement will determine the scattering cross section and polarization transfer coefficients. These observables will be measured both as a function of the four-momentum transfer, over the range of $0.28 \leq Q^2 \leq 1.00$ (GeV/c)^2, and as a function of invariant mass of the intermediate state in the range of 938 MeV $\leq W \leq$ 1150 MeV.

As was argued by Naus et al.[11,12], an opportunity to test our theoretical understanding of the electromagnetic interaction of an off-shell nucleon, free from the above nuclear

complications, is provided by electromagnetic two-step interactions on a free nucleon, such as Compton scattering or pion electro- or photoproduction. The elastic scattering of real photons provides less information than the experiment proposed here. The pion production reaction involves also the structure of $F_{\pi NN}$ vertex and the coupling of the photon into this vertex. VC scattering is the preferred process to start addressing the off-shell effects in the electromagnetic interaction of a nucleon.

Several authors have recently investigated the electromagnetic interaction of an off shell nucleon[11-14]. They have found sizeable effects, with model dependent differences up to 20 % even at moderate Q^2. Clearly the presence of these effects and model dependences have significant implications for the electron scattering experiments planned at CEBAF. A theoretical description of the VC reaction in terms of nucleons with an internal structure must be able to describe the electromagnetic interaction of an off-shell nucleon.

Fig. 1.1 shows some lowest-order Feynman diagrams for the reaction $eN \rightarrow eN\gamma$. They are made up of nucleon electromagnetic vertices, which we are interested in, and the propagator of the intermediate off shell nucleon. These two building blocks are connected by the Ward-Takahashi identity[15]. Not shown are the diagrams that cannot be reduced to these elements, the irreducible diagrams: if the photon-nucleon vertex has structure, e.g. due to a meson cloud, we must also couple the second photon into this vertex.

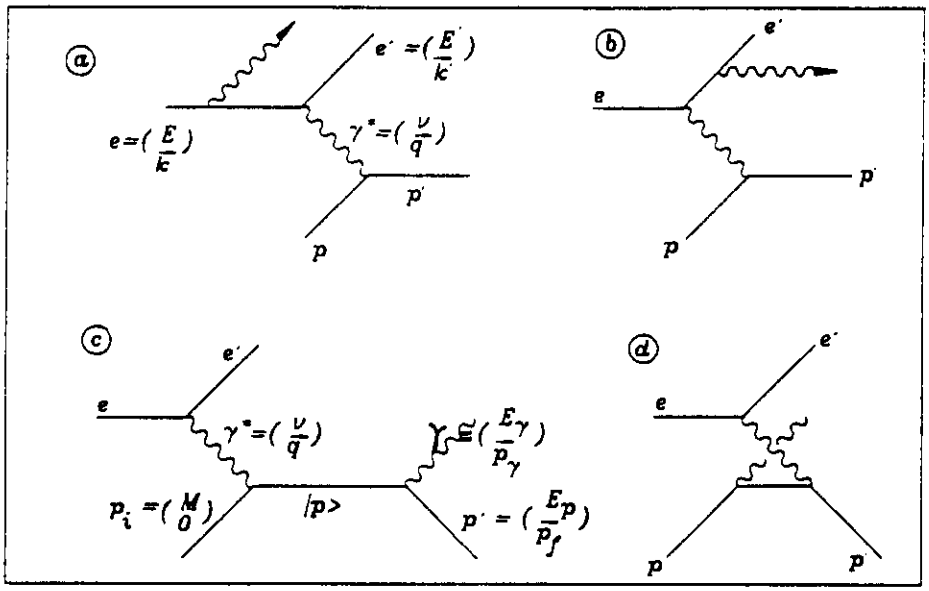

Figure 1.1. *Feynman diagrams representing the Bethe-Heitler (a.b) and Virtual-Compton (c,d) contributions to the reaction* $eN \rightarrow eN\gamma$.

The photon denoted γ^* in Fig. 1.1 is virtual and represents the exchanged field quantum in the interaction of the particle with the electromagnetic field (in lowest order in the fine-structure constant). The other photon, denoted γ, is real. The first two diagrams

represent the dominant case where the photons are radiated by the incoming and outgoing electrons. These diagrams can be calculated to high precision using QED and are termed Bethe-Heitler contributions. The other two diagrams (termed VC contributions) can only be unambiguously calculated in the soft-photon limit, where the cross section is independent of nucleon-structure ambiguities. In general they involve a sum over all possible intermediate hadronic states. The calculation of the VC contribution requires a realistic nucleon model to describe its dynamical behavior and must then also take into account the propagation of intermediate nucleon resonances and other intermediate states. We will show that the proposed reaction is a sensitive probe for this purpose. It may be possible to obtain the required information from the interference of the Bethe-Heitler and VC contributions.

In order to maximize the sensitivity* to the hadronic structure of the nucleon in the reaction $eN \rightarrow eN\gamma$, one has to choose sufficiently large photon energies E_γ to get away from the model independent low-energy predictions for this reaction and select photon emission angles where radiation from the proton is dominant. The reaction allows mapping the observables versus Q^2 and the invariant mass of the intermediate hadronic state, given by

$$W^2 = M^2 + 2E_\gamma(E_p - p_z^f) \tag{1.1}$$

where p_z^f is the component of the outgoing proton momentum along the photon direction. Note that $W^2 > M^2$, so as E_γ increases the role of the Delta resonance becomes increasingly important.

In section II a more detailed scientific justification will be given for the proposed experiment. We will show that measurements of the VC process are feasible with a coincident high-resolution magnetic spectrometers setup, and discuss the sensitivity of the $^1\mathrm{H}(\vec{e}, e'\vec{p})\gamma$ reaction to off-shell effects in a separable model. Details about the experimental setup, such as the proposed cryogenic target and the proton polarimeter, are given in section III. Count rates and run time estimates for the proposed kinematical settings are given in section IV.

* An example of this is real Compton scattering where the leading corrections allow one to measure nuclear polarizabilities.

II. Physics Motivation

2.1. Introduction

The general expression for scattering off a nucleon with both initial and final nuclear momenta off-shell was first given by Bincer[16]. In VC scattering, only one of the nucleons at the electromagnetic vertex is off shell, i.e. the 'half off shell' vertex is involved. If the final nucleon is taken off-shell, the general expression for the half-off-shell vertex[11] is

$$\Gamma_\mu(p',p) = e(\Lambda^+(p')(F_1^{++}\gamma_\mu + \frac{i\sigma_{\mu\nu}q^\nu}{2M}F_2^{++} + q_\mu\frac{(e_N - F_1^{++})(M-W)}{q^2})$$

$$+\Lambda^-(p')(F_1^{-+}\gamma_\mu + \frac{i\sigma_{\mu\nu}q^\nu}{2M}F_2^{-+} + q_\mu\frac{(e_N - F_1^{-+})(W+M)}{q^2})) \qquad (2.1)$$

where e is the elementary charge, e_N is the nucleon charge operator in isotopic-spin space, and $\sigma_{\mu\nu} = (i/2)[\gamma_\mu,\gamma_\nu]$. $F_i^{\rho'\rho}(q^2,M^2,W^2)$ are functions depending on the photon momentum q^2 and on the invariant masses M and W of the incoming and outgoing nucleon with momenta p and p', respectively. The operators Λ^+ and Λ^- project upon positive or negative energy states of mass W. When operating on a free nucleon spinor*, $u(p)$, one has $\Lambda^+u(p) = u(p)$ and $\Lambda^-u(p) = 0$. We have shown equation (2.1) here in its reduced form imposing gauge invariance as expressed through the Ward-Takahashi identity[15].

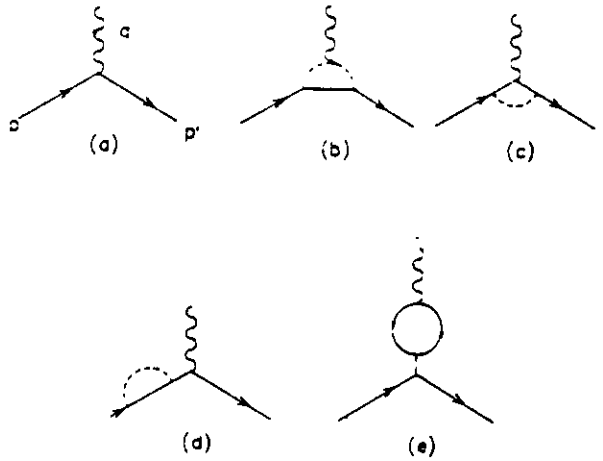

Figure 2.1. *Feynman diagrams for the photon-nucleon vertex to order g^2.*

It is seen that four form factors, dependent on two scalars ($Q^2 = -q^2$ and W^2), are needed for a complete description of the half-off shell vertex. For the on-shell matrix element one easily sees that $F_1^{++}(Q^2,M^2,M^2)$ and $F_2^{++}(Q^2,M^2,M^2)$ become the Dirac

* For a bound nucleon the operators Λ^+ and Λ^- follow from the nuclear dynamics.

and Pauli form factors $F_1(Q^2)$ and $F_2(Q^2)$, respectively. In addition it can be shown[16] that at the photon point one has $F_1^{\pm+}(0, M^2, W^2) = e_N$, while there is no such constraint on the form factors $F_2^{\pm+}$. It is clear that in general the off-shell interaction cannot be extrapolated from the on-shell case and a dynamical model of the nucleon is required in order to calculate $F_1^{\pm+}(Q^2, M^2, W^2)$ and $F_2^{\pm+}(Q^2, M^2, W^2)$.

To study aspects of the electromagnetic interaction of an off-shell nucleon, Naus and Koch[11,12] evaluated these form factors occuring in Eq. (2.1) by using a pion and nucleon field coupled through the pseudoscalar interaction, $L_{\pi NN} = -ig\bar{\psi}\gamma_5\tau \cdot \phi\psi$. This well-known field-theoretical model is known to be renormalizable. The electromagnetic vertex was calculated up to order eg^2. Feynman diagrams of this order are shown in Fig. 2.1.

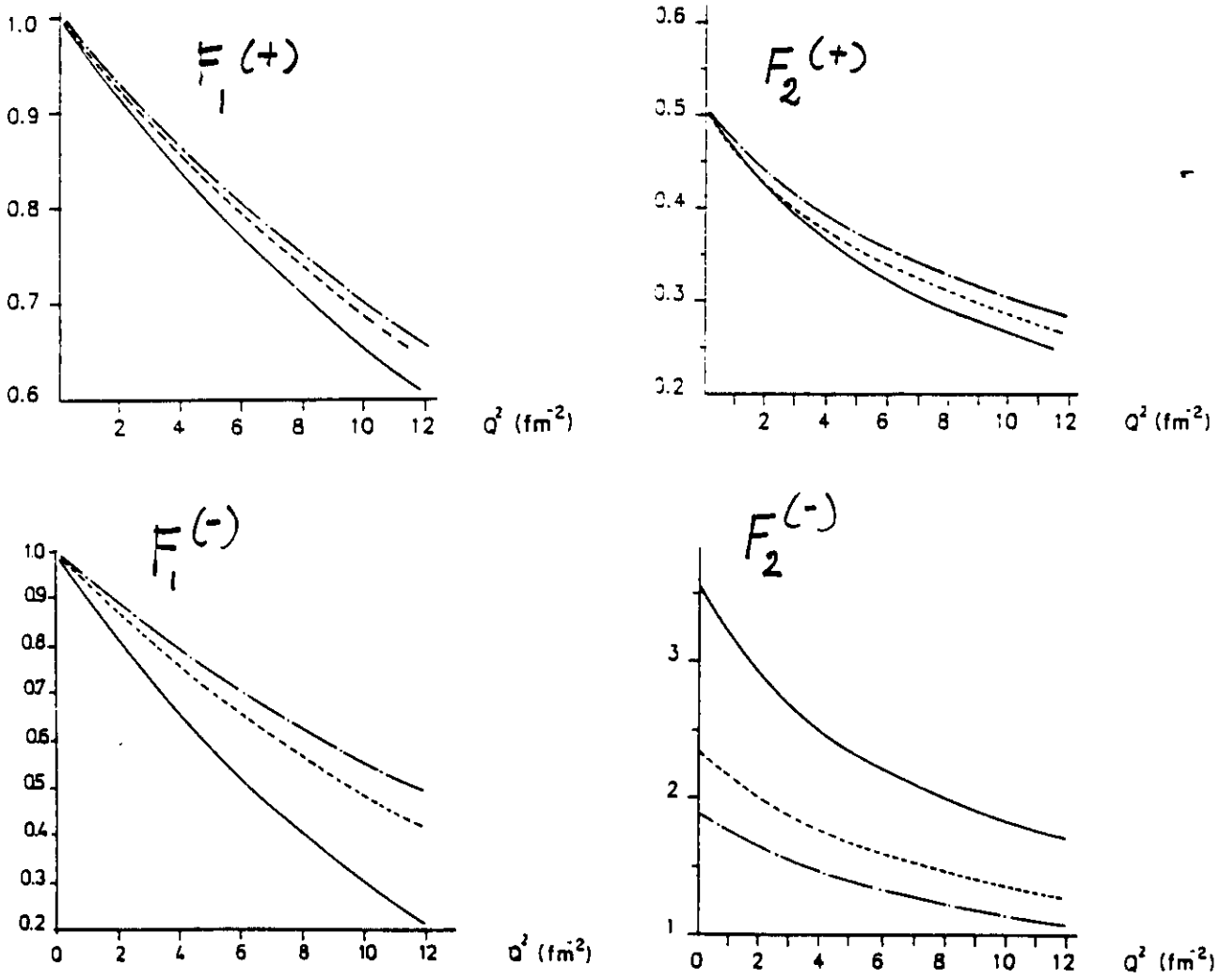

Figure 2.2. *The form factors F_1 and F_2 as function of $Q^2 = -q^2$. Solid curve, $W = M$; dashed, $W = 800$ MeV; dot-dashed, $W = 700$ MeV.*

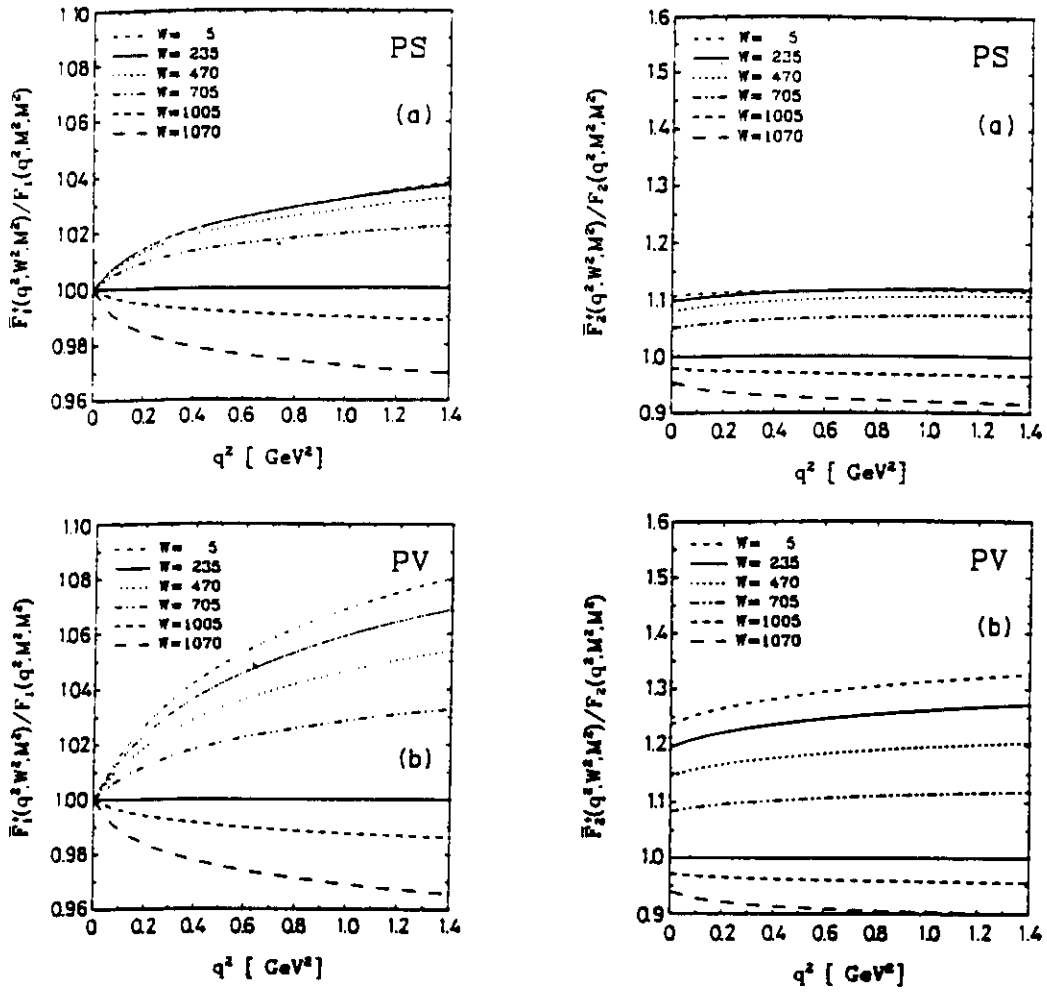

Figure 2.3. *The ratio of the proton rescaled half-off-shell form factor and the on-shell form factor as calculated for pseudoscalar (PS) and pseudovector (PV) coupling.*

Fig. 2.2 shows the predictions for the various structure functions for several off-shell situations. The figure shows that effects up to 30 % are observed for moderate Q^2. In addition, the magnitude of these effects are predicted to increase with increasing Q^2. The calculations correspond to situations encountered in (e,e'p) reactions. In virtual Compton scattering the invariant mass of the intermediate state has $W > M$. Tiemeijer and Tjon[13] calculated off-shell effects for this situation using the one-pion loop corrections to the vector-meson dominance model. Considering both pseudoscalar and pseudovector interactions for the pion-nucleon coupling they found significant effects (up to 10 % at $Q^2 \approx 1$ (GeV/c)^2) in the form factors. We show their results in Fig. 2.3.

With respect to quasi-free scattering, we would like to note that while the half-off-shell vertex (corresponding to $F_{1,2}(Q^2, W^2, M^2)$) is encountered in PWIA, in DWIA the full off-shell vertex (corresponding to $F_{1,2}(Q^2, W^2, W'^2)$) needs to be considered. In principle, this situation holds for the extensive set of inclusive scattering, especially y-scaling, and (e,e'p)

measurements. Calculations by Tiemeijer and Tjon show that the off-shell variations are larger for the full off-shell vertex. The same observation was made by Naus et al.[12].

In summary, the magnitude of the off-shell effects on the form factors and consequently scattering cross sections are predicted to be sizable. In commonly used prescriptions[3], for example in σ_{cc}^1, such effects are not included and the comparison of different 'cc-recipes' gives no valid estimate for the size of the off-shell effects. If the off-shell effects are of the magnitude as predicted in the above discussed microscopic models of the nucleon, then this will have significant consequences for intermediate-energy electron scattering experiments planned at CEBAF. Here, we discuss a possible study of these off-shell effects using virtual Compton scattering as a probe.

2.2. Formalism

The experiment involves the measurement of the cross section and the three components of the proton polarization after being scattered by the incident longitudinally polarized electron. The coordinate system used in describing the $(\vec{e}, e'\vec{p})$ reaction is outlined in Fig. 2.4.

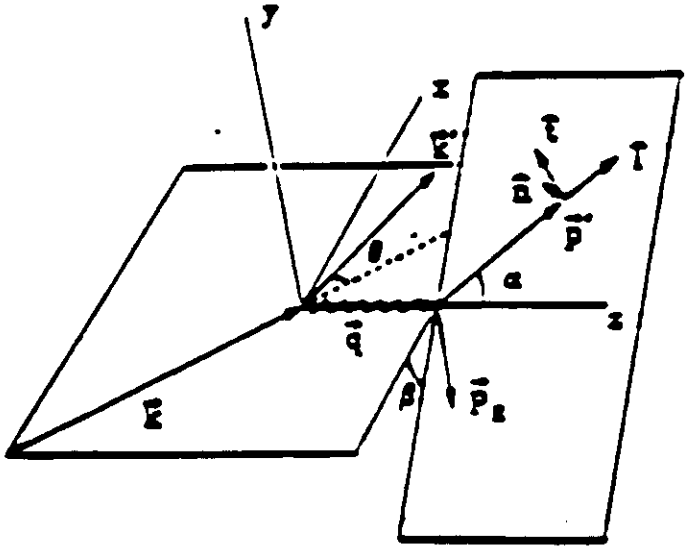

Figure 2.4. *The coordinate system and the various kinematical quantities.* k_0 (k_0') *is the energy of the incident (scattered) electron.* h *is the incident electron helicity and* $\mathbf{q}^2 = Q^2 + \omega^2$.

The unit vectors **n**, **l** and **t**, are defined by choosing **l** parallel to the proton momentum, $\mathbf{n} = (\mathbf{q} \times \mathbf{l})/|\mathbf{q} \times \mathbf{l}|$ and $\mathbf{t} = \mathbf{n} \times \mathbf{l}$, the projection of the spin unit vector onto these basis vectors can be defined as:

$$S_n = \mathbf{n} \cdot \mathbf{s}'_R, \; S_l = \mathbf{l} \cdot \mathbf{s}'_R, \text{ and } S_t = \mathbf{t} \cdot \mathbf{s}'_R. \tag{2.2}$$

The normal component, p_y^0, is helicity independent and vanishes for elastic electron-proton scattering. The transverse component of the recoil polarization, p_x', which is located in the scattering plane is related to the electron beam helicity, h, as:

$$p_x' = hD_{lt}. \tag{2.3}$$

The longitudinal component is given by:

$$p_z' = hD_{ll}. \tag{2.4}$$

We will measure the polarization transfer coefficients for the reaction $^1\mathrm{H}(\vec{e}, e'\vec{p})\gamma$ in off-shell kinematics as function of W^2 and Q^2. They are directly sensitive to the nucleon structure as can be easily shown for the on-shell limit corresponding to elastic electron-proton scattering. Here, the polarization transfer coefficients D_{lt} and D_{ll} can be expressed[17] in terms of the nucleon form factors G_E and G_M:

$$\begin{aligned} I_0 D_{lt} &= -2\sqrt{(\tau(1+\tau)}G_M G_E \tan\theta_e/2 \\ I_0 D_{ll} &= \frac{k_0 + k_0'}{m_p}\sqrt{(\tau(1+\tau)}G_M^2 \tan^2\theta_e/2 \\ I_0 &= G_E^2 + \tau G_M^2[1 + 2(1+\tau)\tan^2\theta_e/2], \end{aligned} \tag{2.5}$$

here $\tau = Q^2/4m_p$. Note that also a ratio R_P can be formed from the proton polarization components p_z' and p_x' which, in the limit $Q^2 \to 0$ and $W \to M$, is directly related* to the magnetic moment of the free proton.

The spin vector of the proton is measured in the polarimeter after it is momentum analyzed in the 4 GeV/c proton spectrometer. Contrary to both the normal and the longitudinal spin components, the sideways component does not precess (in first order) in the magnetic field of the spectrometer. The polarimeter coordinate system is defined as follows: X axis is along the momentum dispersion direction, Y axis is normal to the bend plane and Z axis is along the proton momentum. The polarization components after precession by an angle χ through the 4 GeV/c proton spectrometer are given by:

$$\begin{aligned} p_X &= p_y^0 cos\chi + p_z' sin\chi \\ p_Y &= p_x' \\ p_Z &= -p_y^0 sin\chi + p_z' cos\chi. \end{aligned} \tag{2.6}$$

* One finds that $R_P = -\frac{2m_p}{(k_0+k_0')\tan\theta_e/2}\frac{p_x'}{p_z'} = \frac{G_M}{G_E}$, where R_P does not involve knowledge of the electron polarization, and again the last equality is only true for elastic ep scattering. The systematic error in this ratio is expected to be small as only the accuracy of the incident and scattered electron energies, the scattering angle, and the spin precession angle enter.

The precession angle is given by:

$$\chi = \frac{g-2}{2}\gamma\Omega_B, \tag{2.7}$$

where g is the gyromagnetic ratio of the proton (5.586), γ is the Lorentz factor and Ω_B is the total bend angle in the proton spectrometer (for the central ray $\Omega_B = 45°$).

The focal-plane polarimeter determines therefore p'_x and a combination of longitudinal and normal components, p'_z and p^0_y. The normal component will be separated from p'_z using its independence of the electron helicity. In the on-shell limit p^0_y is expected to be zero.

2.3. Estimates for the Cross Section and Polarization Transfer Coefficients

To gain insight in the sensitivity of the VC scattering process to the nucleon structure, we extended the formalism by Mo and Tsai[18] to coincidence (e,e'p) reactions[19]. The treatment of order e^4 contributions to the virtual-photon correction involving the strong interaction is similar to that of Mo and Tsai.

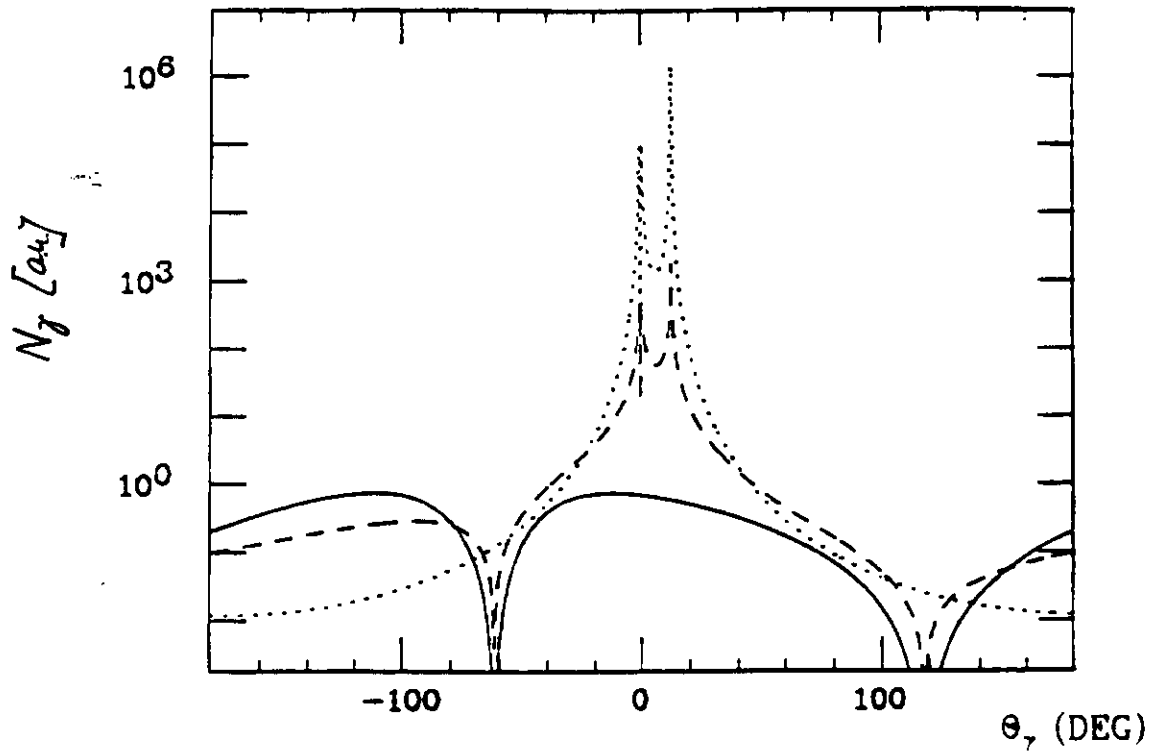

Figure 2.5. *Angular distribution of radiated events for kinematics 3. The various lines denote the δ_{ee} (dotted), δ_{ep} (dashed), and δ_{pp} (solid) contributions.*

The formalism includes the complete half off-shell coupling as given by expression (2.1) which allows a study of the dependence on various models of the nucleon. In addition, the

sensitivity to negative energy states, which was already recognized by Drell more than forty years ago[20], can be investigated. The model contains the approximation of separability which allows for only nucleon intermediate states.

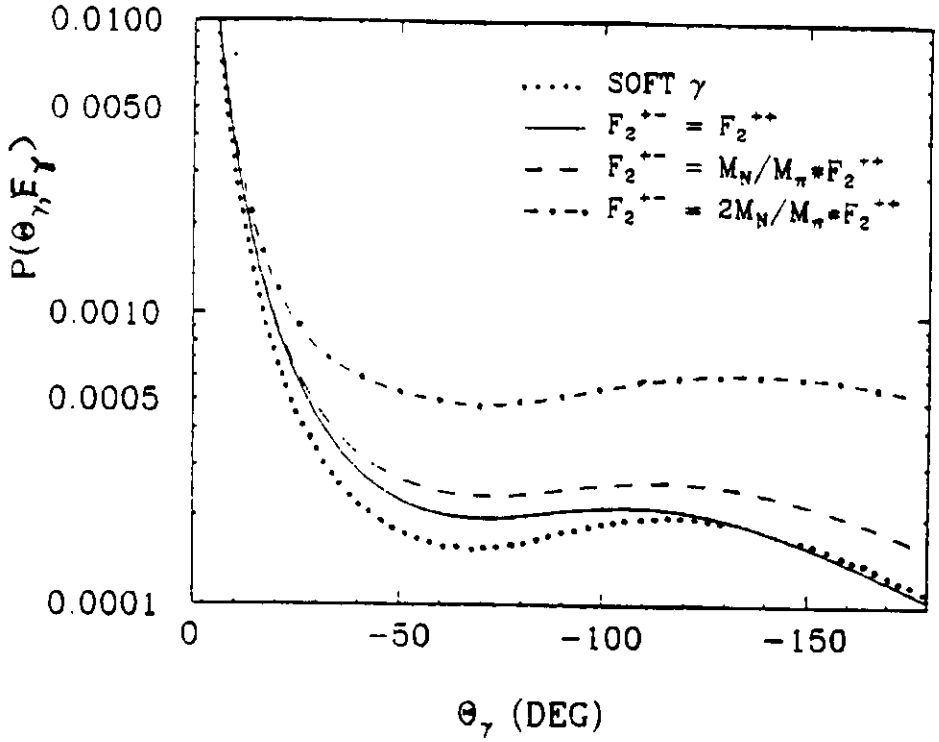

Figure 2.6. *Probability distribution for the emission of photons of 100 MeV energy in the reaction $^1H(e,e'p)$. The various lines denote different nucleon models. as described in the text. A beam energy of 2.51 GeV and an electron scattering angle of 12.5° is assumed.*

Fig. 2.5 shows the angular distributions calculated for kinematics 3 (see section 4.1) in the soft-photon limit. The total radiative effects have been divided into three parts, one solely due to electron radiation (δ_{ee}), one due to the contribution from electron-proton interference (δ_{ep}), and one due to the contribution from direct proton radiation (δ_{pp}) only. It is seen that the radiation from the proton is dominant for photon angles less than -80°. Next, we have applied our model to the measurement of the reaction $ep \rightarrow ep\gamma$ at low Q^2, corresponding to kinematics 1 discussed in section 4.1. Fig. 2.6 shows the probability, $P(\Theta_\gamma, E_\gamma)$, for photon emission for a kinematics with E (E') = 2.51 (2.36) GeV and Q^2 = 0.28 (GeV/c)^2 and for E_γ of 100 MeV. The radiated cross section is defined as

$$\frac{d\sigma}{d\Omega_{e'} dE_\gamma d\Theta_\gamma} = \frac{d\sigma^{(ep)}}{d\Omega_{e'}} \frac{1}{E_\gamma} P(\Theta_\gamma, E_\gamma) \tag{2.8}$$

where $\sigma^{(ep)}$ indicates the electron-proton cross section without any radiation. The dotted curve in Fig. 2.6 shows the result in the soft-photon limit, while the solid curve assumes

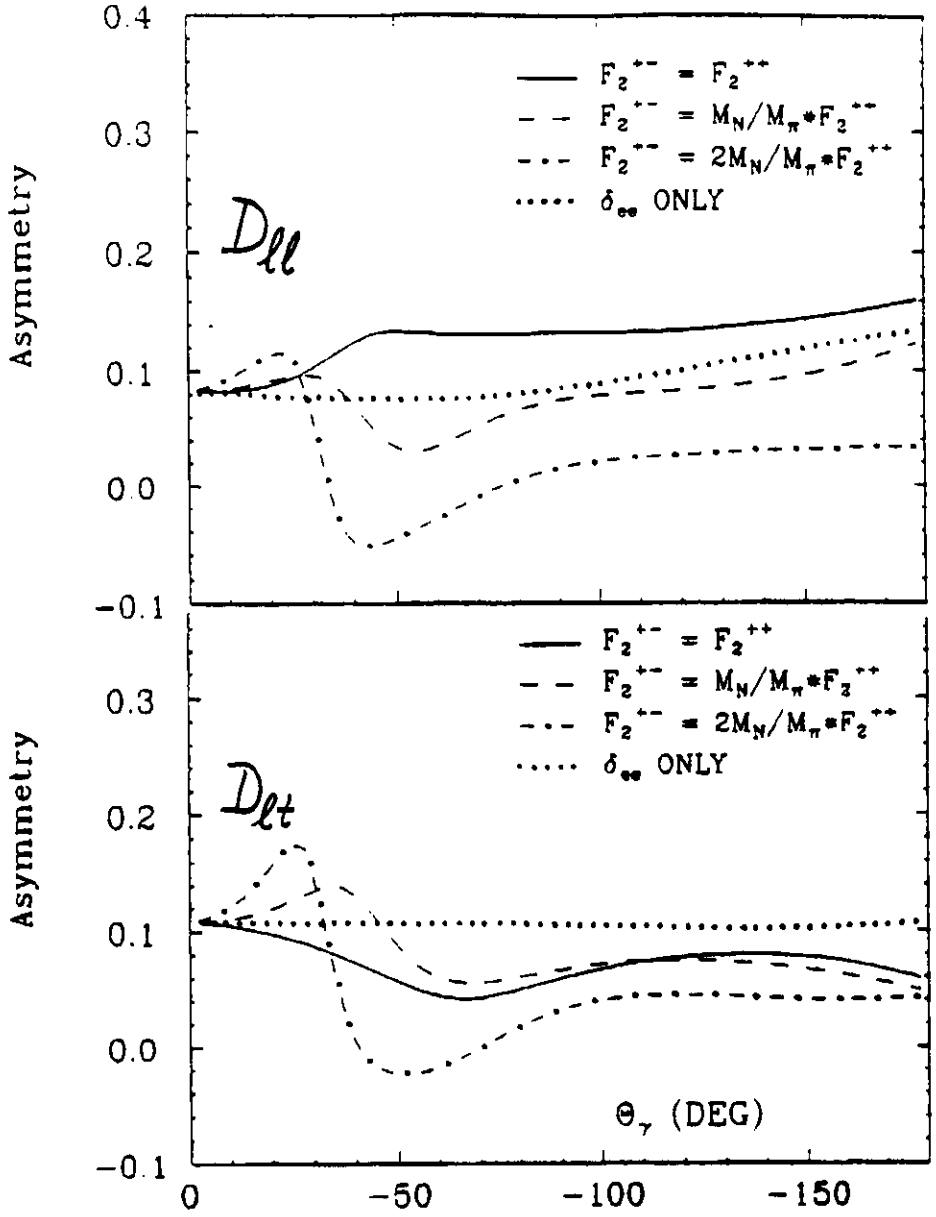

Figure 2.7. *Polarization transfer coefficients D_{ll} and D_{lt} versus photon angle. For a discussion of the various curves see the text.*

F_2^{-+} equal to F_2^{++} (and F_1^{-+} equal to F_1^{++}). The other curves assume a W and Q^2 dependence estimated from the predictions of the one-pion loop model of Ref. 11, and only differ in the relative normalization of $F_2^{-+}(Q^2 = 0)$ to $F_2^{++}(Q^2 = 0)$. The dashed curve assumes a relative normalization of $\approx \frac{M}{m_\pi}$ as given by Ref. 11, whereas the dotdashed curve assumes a relative normalization of $\approx \frac{2M}{m_\pi}$ as derived from dispersion relations[21]. The figure shows that in this kinematic region one is sensitive to the unconstrained form factor F_2^{-+} which measure the anomalous magnetic moment of an off-shell proton. Fig. 2.7 shows the polarization transfer coefficients calculated for the same kinematics. It is seen that the asymmetries are sizable and the sensitivity to hadronic structure effects is large. All models predict the same asymmetry in the limit $\theta_\gamma \to 0$. The asymmetry is greatly

varying around $\theta_\gamma = -30°$. In this region the interference between the Bethe-Heitler and VC contributions is dominant. The results clearly indicate the sensitivity to the nucleon model used in the calculations.

III. The Experiment

3.1 Introduction

The experiment can be carried out at the CEBAF electron-scattering facility using the Hall A spectrometers. An incident electron beam with 100 % duty factor and an energy of 2.5 - 4.0 GeV allows measurements at four-momentum transfer values Q^2 = 0.28, 0.56, and 1.00 $(GeV/c)^2$. The dependence of the cross section can be mapped out as a function of the photon energy up to a value of 150 MeV. The (e,e'γ) reaction can be identified by detecting the scattered electron in coincidence with the proton. This requires the use of the high-resolution spectrometers available in Hall A in order to guarantee a precise reconstruction of the photon kinematics. The anticipated missing-energy resolution is estimated at approximately 1 MeV.

The coincidence detection efficiency can be calibrated with the reaction ^{1}H(e,e'p). The total coincidence yield can be corrected for accidentals and weighed by the detection volume calculated with a Monte Carlo simulation, taking the angular acceptance of the spectrometers as a function of the vertex position into account. During the actual experiment the coincidence yield as a function of the incident electron beam position can be used as a check on the mutual alignment of the spectrometers, beam and target cell.

3.2 The Cryogenic Target

A cryogenic target is being developed by the Hall A collaboration. The LH_2 target will operate at 20 K and a pressure of 3 atm, necessary in order to suppress macro bubble formation. A description of the target system can be found in reference[22]. The target cells will have a length of 10 cm and can operate with beam currents up to 150 μA. The design value for the maximum cooling power amounts 1 kW. For the present experiment we assume a beam current of 100 μA and consequently a moderate level of power dissipation. The resulting luminosity amounts to 2.6×10^{38} e^-atoms $cm^{-2}s^{-1}$.

3.3 Virtual-Compton Scattering Effects.

Experimentally, the reaction $eN \rightarrow eN\gamma$ can be best approached by detecting a scattered electron in coincidence with a proton using high-resolution magnetic spectrometers, under construction in Hall A at CEBAF.

The measurement is complicated due to the fact that an abundance of photons will be radiated by the incoming and scattered electrons. This will lead to radiation tails in the missing-energy and momentum plane, defined by $E_m = \omega - E_{p'} + M$ and $\vec{p_m} = \vec{q} - \vec{p'}$. Fig.

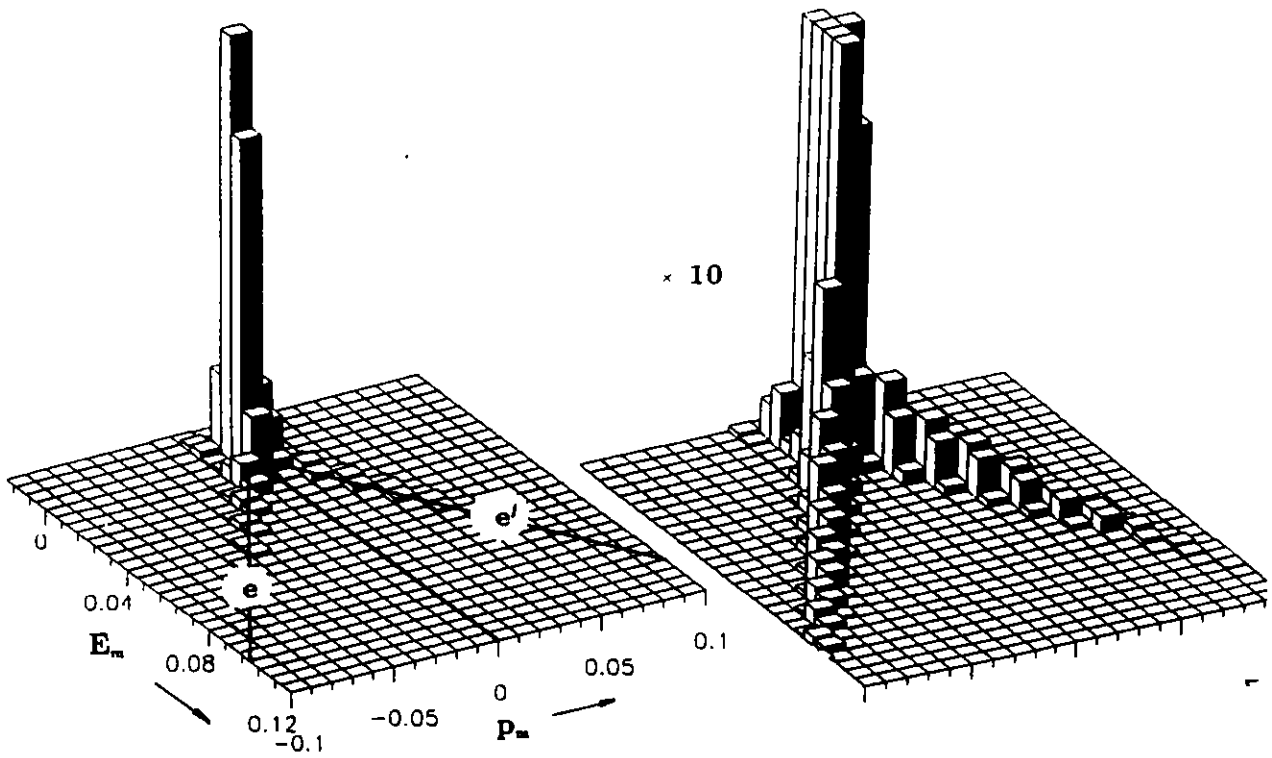

Figure 3.1. *Not-unfolded spectral function for the reaction $^1H(e,e'p)$, where the two radiative tails due to radiation of the electron before and after the interaction can be observed. The sign of $\vec{p_m}$ is + (-) in case the angle of $\vec{p_m}$, with respect to the incident electron, is < (>) tan$\theta/2$.*

3.1 demonstrates this effect with the data recently obtained by the NE-18 collaboration[23] at SLAC for the reaction ^{1}H(e,e'p), for an incident (scattered) electron energy of 2.015 (1.400) GeV and consequently Q^2 = 1.15 (GeV/c)^2. The tails due to radiation of the incident and scattered electrons are readily observed.

The angular distribution of the count rate is shown in Fig. 3.2. For the data the photon angle has been reconstructed from the measured $\vec{p_m}$. The invariant mass of the photons can be reconstructed from the kinematics and was in the range -0.01 $\leq W_\gamma^2 \leq$ 0.002 GeV^2. Thus, VC events are well separated from the pion production contributions. A cut has been applied to select only photons with $E_\gamma > 40$ MeV, resulting in a range of invariant mass of the intermediate hadronic state of $M \leq W \leq 1060$ MeV. It is seen that the radiation is dominant in the direction of the initial and final electrons, where narrow peaks are seen in accordance with the peaking approximation[24].

In Fig. 3.3. we show the number of radiated events in the interval $-60° < \theta_\gamma < -20°$

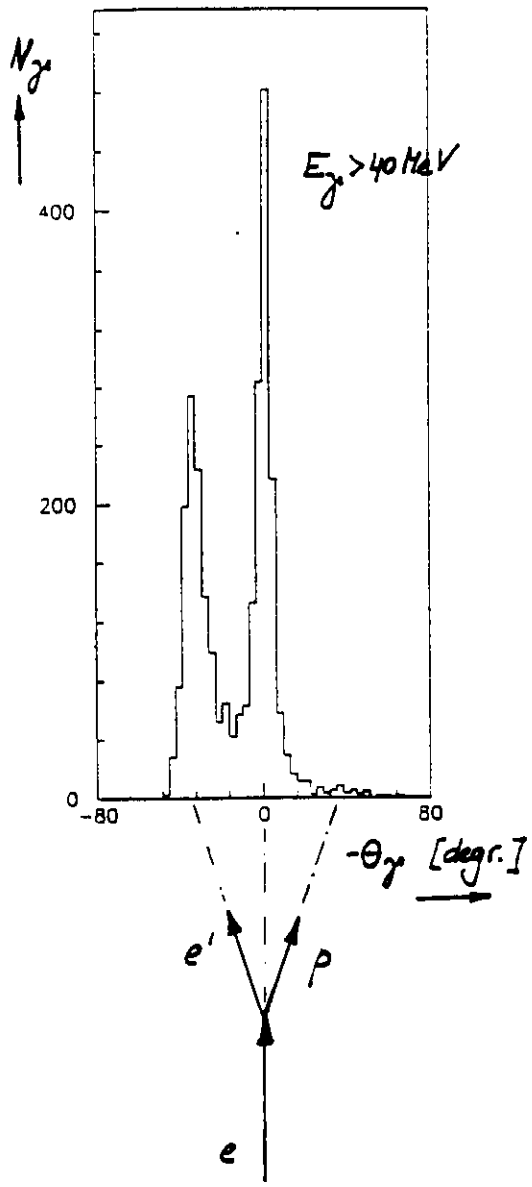

Figure 3.2. *Angular distribution of radiated events obtained at NE-18 for* $E_\gamma > 40$ *MeV.*

obtained at NE-18 versus the cut-off energy E_γ. The solid (dashed) curve shows the prediction in the soft-photon limit for Bethe-Heitler and VC contributions (Bethe-Heitler only). The agreement between data and prediction of the number of counts when proton radiation is included clearly demonstratesthe experimental viability of the technique even with the 2×10^{-4} duty factor available at the SLAC end-station. However, the number of counts in this regime is too low to allow for a meaningful study of the nucleon structure.

3.4 The focal-plane proton polarimeter

The focal-plane proton polarimeter for the 4 GeV/c proton spectrometer in Hall A is being developed by the Hall A collaboration. A full description of this polarimeter

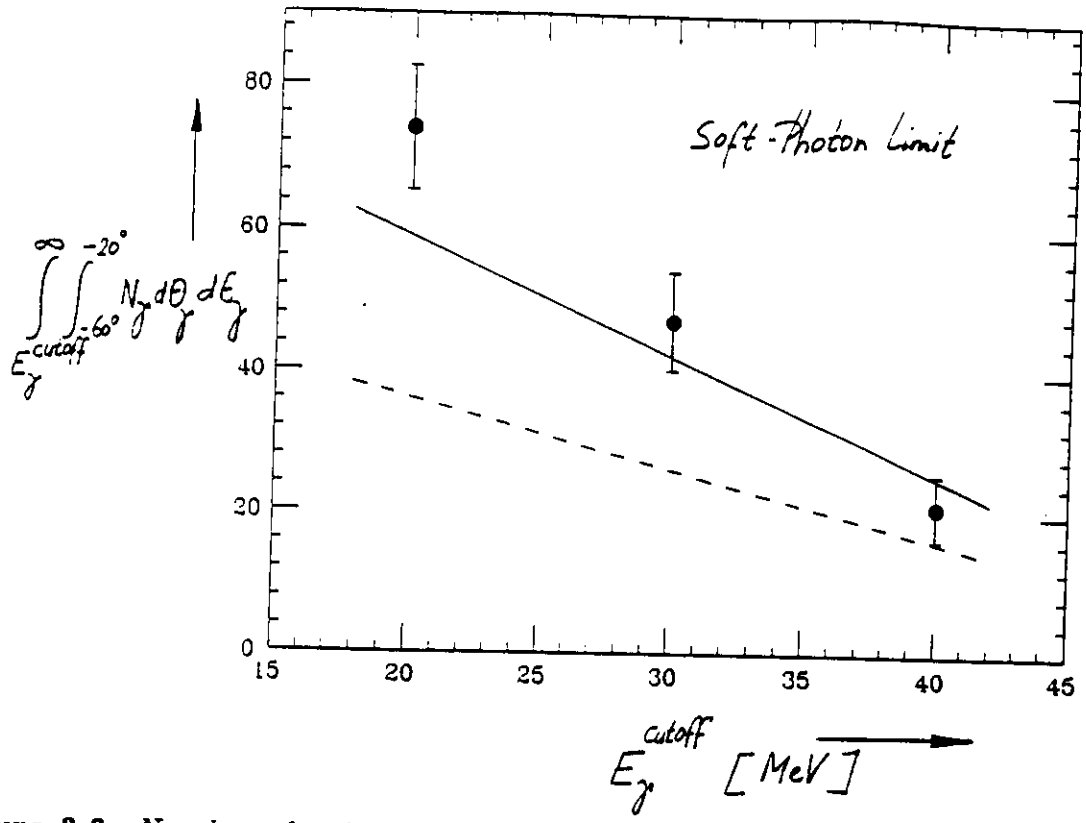

Figure 3.3. *Number of radiated events in the interval* $-60° < \theta_\gamma < -20°$ *obtained at NE-18 versus the cut-off energy* E_γ. *The solid (dashed) curve shows the prediction in the soft-photon limit for Bethe-Heitler and VC contributions (Bethe-Heitler only).*

can be found elsewhere[22]. The design is based on existing technology and is similar to polarimeters already in use at LAMPF, IUCF, TRIUMF, and SATURNE. The design uses a graphite analyzer preceeded and followed by a series of straw drift chambers.

IV. Count-Rate and Running-Time Estimates

4.1 Kinematics

The kinematics are given in Table 1 and are chosen such as to determine the dependence of the observables as a function of the four-momentum transfer, over the range of 0.28 to 1.00 $(GeV/c)^2$. In each setting the dependence on the invariant mass of the intermediate state will be measured from 938 to about 1150 MeV. The polarimeter only determines p'_x and a combination of p^0_y and p'_z. The latter two contributions can be separated through the use of the electron helicity.

4.2 Count Rate Estimates

For count-rate estimates we have assumed the following spectrometer acceptances: 10 % in momentum and a solid angle of 7.8 msr. As both spectrometers will see the total length (10 cm) of the extended target, a target thickness of 0.7 g·cm^{-2} has been used in the estimates.

Coincidence rates are given in Table 2, assuming an average current of 100 μA. We have selected only photons emitted by the δ_{pp} contribution in a certain missing-energy interval in our count-rate estimates. Here, we have integrated over a photon angular range of about $\Delta\theta = 60°$. A similar integration range was assumed for the out-of-plane angle ϕ, and a flat response as a function of that angle.

For the $Q^2 = 0.28$ and 0.56 $(GeV/c)^2$ kinematics, it is possible to obtain a 2% statistical error, for a bin of 10 MeV bin in photon energy and 10° in photon angle, within 20 hours of beam time. A 3% statistical error, in a similar bin for the $Q^2 = 1$ $(GeV/c)^2$ kinematics, requires 40 hours of beam time. A total amount of 130 hours of beam time seems appropriate for a first unpolarized measurement. This estimate includes checkout and calibration of the experimental setup.

Next we estimate the running-time required for a measurement of the polarization transfer coefficients. To calculate the statistical precision only those coincidence events which scatter usefully in the focal-plane polarimeter should be considered. The cross section for scattering a polarized electron from an unpolarized proton followed by a second scattering of the outgoing polarized proton from an analyzer is (for parallel kinematics):

$$\sigma = \sigma_0[1 + p'_x A_y sin\phi_2 + (p^0_y cos\chi + p'_z sin\chi)A_y cos\phi_2], \qquad (4.1)$$

where ϕ_2 is the azimuthal angle of the secondary scattering, A_y is the analyzing power, σ_0 is the unpolarized cross section and χ is the precession angle in the proton spectrometer.

By measuring the ϕ_2 distribution in the polarimeter one can disentangle the polarization component p'_x from the other polarization component, which is a combination of p^0_y and p'_z. The statistical uncertainty in either polarization component is:

$$\Delta p_i = \frac{\pi}{2\bar{A}_y}\sqrt{\frac{1}{fN}}, \tag{4.2}$$

where A_y is the analyzing power averaged over an angular cone for which A_y is substantially different from zero, f is the fraction of events that scatter into this cone and N is the total number of events detected in the spectrometer focal plane.

Shown in Table 3 are the assumed polarimeter parameters for each kinematics. Table 4 shows the run times. For the longitudinal polarization of the incident electrons we assume 40 %.

4.3 Beam Time Request

The total beam time required is 480 hours, including 50 hours for setting up and testing the experimental apparatus (see Table 5). The proposed measurements will give an accurate experimental value of the polarization transfer coefficients with a statistical uncertainty better than 0.03, 0.02, and 0.03, for Q^2 of 0.28, 0.56, and 1.00 $(\mathrm{GeV/c})^2$, respectively. The estimate of this uncertainty is partly dependent on the model used to estimate the cross section and polarization transfer coefficients for the $^1\mathrm{H}(\vec{e}, e'\vec{p})\gamma$ reaction.

In summary, a measurement of the virtual Compton scattering cross section in the reaction ^{1}H(e,e'p)γ allows a precise study of the off-shell electron-proton vertex. The dependence of the cross section can be measured both as a function of the four-momentum transfer, over the range of 0.28 to 1.00 $(\mathrm{GeV/c})^2$, and as a function of invariant mass of the intermediate state in the range of 938 to about 1150 MeV. We have shown that this allows for precise tests of microscopic models for the nucleon.

The experimental technique will have sensitivity to new structure functions, beyond $F_1(\mathrm{Q}^2)$ and $F_2(\mathrm{Q}^2)$, which are required for a correct description of the off-shell vertex. The proposed experimental method allows measurement of the off-shell behavior, free from obscurance due to nuclear-structure, final-state interaction and meson-exchange currents effects.

Table 1. *Kinematics for $^1H(e,e'p)\gamma$ experiment. The settings given correspond to central (e,p) elastic scattering kinematics.*

Kin	E	Q^2	E'	p'	θ_e	θ_p
	[GeV]	[$(GeV/c)^2$]	[GeV]	[GeV/c]	[degr]	[degr]
1	2.51	0.28	2.36	0.55	12.50	-68.06
2	3.60	0.56	3.30	0.81	12.50	-62.09
3	4.00	1.00	3.47	1.14	15.47	-54.44

Table 2. *Estimated coincidence counting rates for the proposed kinematics; integrated over a photon angular range of about 60°.*

Kin	Q^2	E_γ	N_C
	[$(GeV/c)^2$]	[MeV]	[Hz]
1	0.28	20 - 50	108
1	0.28	50 - 100	80
2	0.56	20 - 50	45
2	0.56	50 - 100	33
2	0.56	100 - 150	20
3	1.00	20 - 50	10
3	1.00	50 - 100	7
3	1.00	100 - 150	4

Table 3. *Assumed polarimeter parameters. The quoted polarization components correspond to the on-shell case.*

Kin	Anal. thickness [cm]	A	f	D_{ll}	D_{lt}
1	3	0.34	0.006	0.10	0.10
2	10	0.47	0.04	0.15	0.12
3	25	0.32	0.15	0.20	0.15

Table 4. *Estimate for the required beam time for the polarized (unpolarized) measurements.*

Kin	E [GeV]	Q^2 [$(\mathrm{GeV}/c)^2$]	Time [Hours]
1	2.51	0.28	150 (20)
2	3.60	0.56	100 (20)
3	4.00	1.00	100 (40)

Table 5. *Beam time request.*

	Time [hours]
Setup and Checkout	50
Data Acquisition	430
TOTAL	480

References

* On leave from the University of Wisconsin, Madison, WI 53607, USA.

1. T. de Forest, Jr. and J.D. Walecka, Adv. Phys. **15**, 1 (1966).
2. B. Frois and I. Sick, *Modern Topics in Electron Scattering*, World Scientific (1991).
3. T. de Forest, Jr., Nucl. Phys. **A392**, 232 (1983).
4. L.S. Celenza, A. Pantziris, C.M. Shakin, and Hui-Wen Wang, Phys. Rev. **C41**, 176 (1990).
5. L.Ya. Glozman, V.G. Neudatchin, I.T. Obukhovsky, and A.A. Sakharuk, Phys. Lett. **B252**, 23 (1990); Sov. J. Nucl. Phys. **55**, 1491 (1992).
6. P.J. Mulders, and A.E.L. Dieperink, Nucl. Phys. **A483**, 621 (1988).
7. W. Bentz *et al.*, Nucl. Phys. **A436**, 593 (1985).
8. P.J. Mulders in the Book *Modern Topics in Electron Scattering*, Eds. B. Frois and I. Sick, World Scientific (1991).
9. W. Bertozzi, R.W. Lourie, and E.J. Moniz in the Book *Modern Topics in Electron Scattering*, Eds. B. Frois and I. Sick, World Scientific (1991).
10. EMC Collaboration, J.J. Aubert *et al.*, Phys. Lett. **B123**, 275 (1983).
11. H.W.L. Naus and J.H. Koch, Phys. Rev. **C36**, 2459 (1987); Phys. Rev. **C44**, 3445 (1991).
12. H.W.L. Naus, S.J. Pollock, J.H. Koch and U. Oelfke, Nucl. Phys. **A509**, 717 (1990).
13. P.C. Tiemeijer and J.A. Tjon, Phys. Rev. **C42**, 599 (1990).
14. X. Song, J.P. Chen, and J.S. McCarthy, J. Phys. G: Nucl. Part. Phys. **17**, L75 (1991); Z. Phys. **A341**, 275 (1992).
15. Y. Takahashi, Nuovo Cimento **6**, 371 (1957).
16. A.M. Bincer, Phys. Rev. **118**, 855 (1960).
17. R.G. Arnold *et al.*, Phys. Rev. **23**, 363 (1981).
18. L.W. Mo and Y-S. Tsai, Rev. Mod. Phys. **41**, 205 (1969).
19. D. Wasson, R. Ent, N. Makins, and R. Milner, to be published.
20. S.D. Drell, Phys. Rev. **87**, 753 (1952).
21. E.M. Nyman, Phys. Rev. **170**, 1628 (1970); Nucl. Phys. **A160**, 517 (1971).
22. Conceptual Design Report, Basic Experimental Equipment, CEBAF (1990).
23. Experiment NE-18 at SLAC, Spokesman: R.G. Milner and R.D. McKeown (1991). The data were taken in order to calibrate the coincidence detection setup. A 2 μA electron beam was incident on a 4 cm LH_2 target. A total of 5×10^4 counts were measured in 4 hours of running time.
24. L.I. Schiff, Phys. Rev. **87**, 750 (1952).

HAZARD IDENTIFICATION CHECKLIST

CEBAF Experiment: _____ Date: April 14, 1994

Check all items for which there is an anticipated need—do not check items that are part of the CEBAF standard experiment (HRSE, HRSH, CLAS, HMS, SOS in standard configurations).

Cryogenics
- _____ beamline magnets
- _____ analysis magnets
- X target
- _____ drift chambers
- _____ other

Electrical Equipment
- _____ cryo/electrical devices
- _____ capacitor banks
- _____ high voltage
- _____ exposed equipment

Radioactive/Hazardous Materials
List any radioactive or hazadorous/ toxic materials planned for use:
_____
_____

Pressure Vessels (cell)
- ~2 cm inside diameter
- 4 Atm operating pressure
- Al 7075-T6 window material
- ~5 mils window thickness

Flammable Gas or Liquids
(incl. target)
- type: LH_2
- flow rate: _____
- capacity: _____

Other Target Materials
- ___ Beryllium (Be)
- ___ Lithium (Li)
- ___ Mercury (Hg)
- ___ Lead (Pb)
- ___ Tungsten (W)
- ___ Uranium (U)
- ___ Other (list below)

_____
_____

Vacuum Vessels
- _____ inside diameter
- _____ operating pressure
- _____ window material
- _____ window thickness

Radioactive Sources
- _____ permanent installation
- _____ temporary use
- type: _____
- strength: _____

Large Mech. Structure/System
- _____ lifting devices
- _____ motion controllers
- _____ scaffolding or elevated platforms
- _____ other

Lasers
- type: _____
- wattage: _____
- class: _____

Installation
- _____ permanent
- _____ temporary

Use
- _____ calibration
- _____ alignment

Hazardous Materials
- ____ cyanide plating materials
- ____ scintillation oil (from)
- ____ PCBs
- ____ methane
- ____ TMAE
- ____ TEA
- ____ photographic developers
- ____ other (list below)

_____
_____
_____

Notes:
_____
_____
_____
_____
_____
_____